

Test Experience, 490-N High-Performance [321-s Specific Impulse] Engine

L. Schoenman,* S. D. Rosenberg,* and D. M. Jassowski†
Aerojet, Sacramento, California 95813-6000

The technology readiness of a new class of high-performance Earth-storable bipropellant engines has been demonstrated at the 490-N thrust level. These new-generation engines derive their high performance from a fine pattern platelet injector and a high-temperature iridium/rhenium chamber, in combination with a regenerative thermal management system that eliminates 1) the need for performance degrading and spacecraft contaminating fuel film cooling and 2) undesirable hot front-end attachments. The iridium-coated rhenium chamber greatly increases the thermal margin over existing engine designs, which use disilicide-coated columbium thrust chambers, by increasing the allowable operating temperature to 2204°C (4000°F). The companion technologies for providing metallurgical joints between the different materials used for the injector, chamber, and high area ratio skirt have been demonstrated and incorporated into flight-type engine designs. Hot-fire test results for the nitrogen tetroxide/monomethylhydrazine bipropellant combination are presented for several engine configurations. An all-welded engine assembly tested in vacuum at the 286:1 area ratio confirmed the performance projection of 321 lbf-s/lbm for the engine and the thermal model, indicating a 315°C (600°F) design margin for the chamber based on maximum engine operating temperature and an acceptable postfire heat soak.

Nomenclature

e	= emissivity
I_{sp}	= specific impulse, pounds force/(pounds mass/s)
MR	= mixture ratio, mass oxidizer/mass fuel
P_c	= chamber pressure
ϵ	= nozzle area ratio, exit area/throat area
σ	= standard deviation

Introduction

THE propellant used for orbit insertion and attitude control is the largest single item contributing to the mass of most spacecraft, e.g., telecommunications satellites. Not only does this increase the cost of placing the satellites in orbit, but the depletion of propellant generally limits satellite life. Any design improvements that can decrease satellite propellant requirements and/or make more effective use of the on-board propellants has significant economic benefit.

The rocket engines generally in use in today's satellites are either relatively low-performing hydrazine monopropellant thrusters or liquid bipropellant engines employing nitrogen tetroxide (NTO) and monomethylhydrazine (MMH) as propellants. The bipropellant engine-delivered performance is considerably lower than theoretically attainable because of the way the combustion chamber is forced to operate due to material limitations. Today's low-thrust engines [under 4450 N (1000 lbf) thrust] employ disilicide-coated columbium alloy chambers that have a nominal upper-use temperature of 1315°C (2400°F) with approximately 10 h of life. To maintain the chamber walls at or below this temperature, a significant amount of the fuel is injected onto the chamber wall as fuel film coolant that does not burn completely before exiting the chamber. In addition to degrading performance efficiency, the unburned fuel represents a source of plume contaminants

that have an adverse effect on sensors, solar cells, and on-board instruments. The amount of fuel film cooling required to maintain acceptable wall temperatures is typically 15–30 wt% for 490-N class engines.

Two new technologies are required in order to obtain the maximum possible performance from these bipropellant engines. The first is an oxidation-resistant material system that can operate at temperatures in excess of 2204°C (4000°F) for tens of hours. The second is a method of attaching the chamber to the injector without overheating the injector and valve and transferring an excessive amount of heat to the engine/spacecraft interface. The injector must be maintained at a temperature low enough to prevent oxidizer vapor lock. The valve must be maintained below temperatures that may damage its soft goods. This head-end temperature limitation is in the 121°C (250°F) range.

This new class of engines is capable of operating at combustion efficiencies that approach 100% without compromising thermal design margin, front-end thermal control, or approaching the upper temperature operating limits of the combustion chamber wall.

Engine Description

The all-welded AJ10-221 490-N engine assembly is shown in Figs. 1 and 2.

Valve

The engine employs a highly reliable bipropellant torque motor valve that is free of sliding or rubbing surfaces that can bind, induce wear, or generate contamination. Valves of this type are flight qualified. They have been produced by the thousands and have demonstrated the ability to deliver over 1,000,000 cycles without sticking, leaking, or shifting the oxidizer-fuel lead-lag relationships on engine startup and shutdown.

Injector

The engine employs a platelet injector design that includes 92 preatomized splash-plate elements.¹ The injector is fabricated from CRES 347 using a photochemical machining and diffusion bonding process. Stainless steel platelet injectors have been life-tested for 40 h² at the 5- and 15-lbf levels and

Presented as Paper 92-3800 at the AIAA/SAE/ASME/ASME 28th Joint Propulsion Conference and Exhibit, Nashville, TN, July 6–8, 1992; received March 25, 1993; revision received Dec. 9, 1994; accepted for publication Dec. 12, 1994. Copyright © 1992 by Aerojet. Published by the American Institute of Aeronautics and Astronautics, Inc., with permission.

*Technical Principal, P.O. Box 13222, Associate Fellow AIAA.

†Chief Scientist, P.O. Box 13222, Member AIAA.

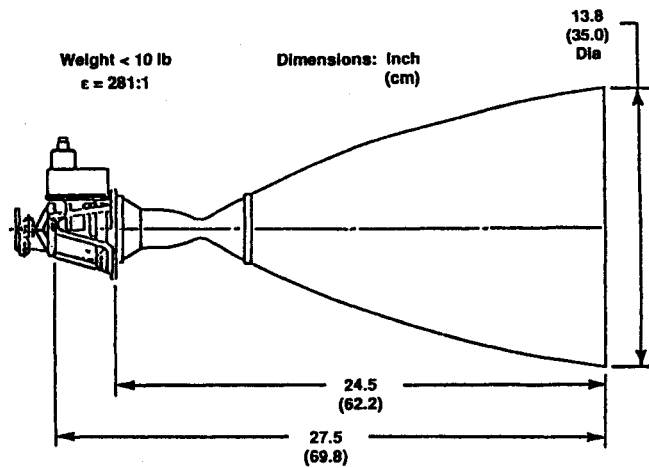


Fig. 1 Envelope of AJ10-221 engine with 286:1 skirt and optional gimbal.

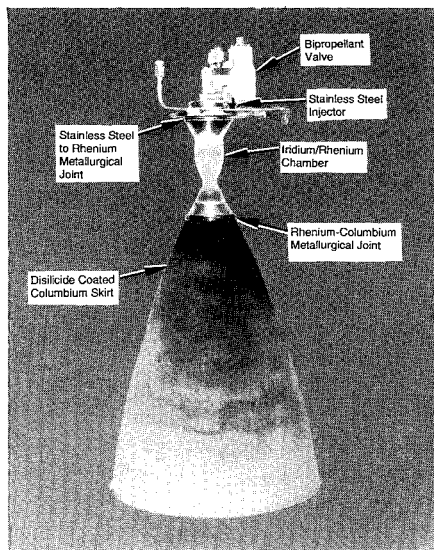


Fig. 2 AJ10-221 all metallurgically joined engine assembly post-hot-fire test.

6 h at the 100-lbf thrust level.³ In the preatomized design, the propellant leaves each injection orifice in an atomized state. The preatomized element eliminates the problem of requiring perfect alignment/impingement of two small diameter liquid streams for the purpose of propellant atomization. Misalignment of small impinging propellant jets is a major cause of nonreproducible engine-to-engine performance, thermal streaking, and poor stability characteristics. The AJ10-221 has an integral critically damped acoustic resonator cavity as part of its basic injector design. The combination of a very large number of short length/diameter (L/D) orifices and the acoustic resonator cavity provides a robust, stable design that is insensitive to flow decay that may be caused by the presence of ferric salts in the oxidizer.

Combustion Chamber

An iridium-lined rhenium combustion chamber allows operation in a simple radiation-cooled mode, without fuel film cooling. Rhenium was selected because it provides good low-temperature ductility and has a melting point 3180°C (5756°F) that exceeds the maximum combustion temperature of the NTO/MMH bipropellant combination by more than 260°C (500°F). The liner, iridium, was selected because of its chemical inertness, i.e., excellent oxidation and oxygen diffusion resistance, high melting point 2454°C (4449°F), and expansion

coefficient that is nearly the same as that of rhenium. The close thermal expansion match of the coating with the substrate eliminates the high-temperature-induced thermal cycle life limitations exhibited by the disilicide-coated columbium system in which the expansion rates of the two materials are significantly different.

The measured equilibrium operating temperature for the AJ10-221 is 1866°C (3390°F) at a combustion efficiency of 99%. This is the highest chamber temperature and it occurs when all of the propellant is fully burned. As discussed in Refs. 1 and 2, a minimum life of 15 h has been demonstrated at 4000°F, without failure, over a wide range of operating conditions, e.g., mixture ratios and chamber pressures. The 321°C (610°F) design margin allows the use of radiation shields, if required by the spacecraft design, without exceeding the demonstrated operating temperature capabilities of the engine.

Nozzle Extension

In order to reduce engine weight and cost, a metallurgically joined disilicide-coated C103 columbium nozzle extension is attached starting at an area ratio of 16:1 to provide the engine with a 286:1 expansion ratio. The rhenium and columbium have nearly identical expansion coefficients, thereby avoiding thermally induced fatigue stresses. This joint operates conservatively at an experimentally verified temperature of 1038°C (1900°F). More than 35 engine firings and a 6-h thermal simulation at 1177°C (2150°F) have validated the durability of this joint design.

Design Validation

Design validation has been obtained by the hot-fire testing of the individual components, i.e., valve, injector, and chamber in a bolt-together 1.68:1 area ratio assembly at sea level, by altitude testing at a 44:1 area ratio with a mechanically attached nozzle extension, and by the hot-fire testing of the complete metallurgically joined assembly at an area ratio of 286:1, as shown in Fig. 2. Additional subscale and life-cycle simulation testing of materials and critical joints has validated the design for a minimum life of 15 h and 1000 full thermal cycles. Table 1 summarizes the validation test history.

Joint Validation

Six subscale stainless steel-to-rhenium joints were fabricated, leak tested, and proof-pressure tested to 1000 psi. All samples passed proof and helium leak checks. Two burst-tested joints exhibited a capability for withstanding pressures of 34.5 MPa (5000 psi). Thermal cyclic-induced strains were predicted to be the ultimate failure mode because of the difference in thermal expansion coefficients of these two materials. Four joints were thermal cycled from 65 to 343°C (150 to 650°F), which is 163°C (325°F) greater than will be experienced in actual engine operation. The designs exhibited an operational capability of more than 1000 thermal cycles without leaking or degrading.

Six rhenium-to-columbium joints that simulated the chamber nozzle extension interface were fabricated and subjected

Table 1 490-N engine validation test history

Component	Quantity	Time, h	Cycles
Injector	3	5.9	240
Regen circuit	3 ^a	6.1	186
Ir/Re chamber	3 ^a	6.1	168
Full assembly	1	0.27	20
Ir/SS ^b joint	6	>24	>1000
Re/Cb ^c joint	6	6	15
Ir/Re subscale	1	15	70

^aOne additional unit has been fabricated and remains untested. Most of the firing time is on a single assembly.

^bStainless steel.

^cColumbian.

Table 2 44:1 Performance for injectors S/N 6-1 and S/N 6-2

Run no.	Injector	Firing time, s	Pc, psia	MR, O/F	$^{\circ}\text{F}_{\text{vac}}$, lbf	I_{vac} , s @ 44:1	Regen. outlet, $^{\circ}\text{F}$	Regen. delta T, $^{\circ}\text{F}$	Regen. heat trans., Btu/s	Chamber temperature, $^{\circ}\text{F}$ ^a
225	S/N6-2	27.0	100.5	1.516	101.3	308.1	166	116	10.8	3514
226	S/N6-2	25.0	100.2	1.662	101.4	309.6	181	132	11.7	3638
227	S/N6-2	25.0	100.2	1.675	101.5	309.7	184	136	12.0	3635
228	S/N6-2	25.0	99.5	1.648	100.7	309.6	180	133	11.8	3631
229	S/N6-2	25.0	110.2	1.620	111.7	308.8	163	116	11.5	3438
230	S/N6-2	25.0	90.5	1.632	91.5	309.7	193	147	12.0	3824
231	S/N6-2	25.0	100.8	1.505	101.5	308.0	166	120	11.4	3487
232	S/N6-2	25.0	100.6	1.788	102.3	310.3	192	146	12.5	3719
233	S/N6-2	25.0	100.5	1.637	101.7	309.8	176	131	11.8	3621
234	S/N6-1	25.0	101.4	1.716	102.8	310.0	188	138	12.1	—
235	S/N6-1	25.0	101.2	1.620	102.3	309.6	180	131	11.9	3704
236	S/N6-1	25.0	100.5	1.647	101.7	309.8	184	135	12.1	3734
237	S/N6-1	25.0	97.4	1.530	98.2	308.6	175	127	11.5	3669
238	S/N6-1	10.8	108.6	1.571	109.6	308.4	159	111	11.0	3204
239	S/N6-1	25.0	107.6	1.576	108.7	308.8	170	122	12.0	3546
240	S/N6-1	25.0	89.6	1.553	90.2	308.6	193	146	12.1	3862
241	S/N6-1	25.0	98.7	1.413	99.1	306.4	163	116	11.2	3510
242	S/N6-1	25.0	98.6	1.720	100.1	310.4	194	147	12.6	3844
243	S/N6-1	10.0	95.8	1.467	96.1	307.0	167	120	11.0	3333
244	S/N6-1	90.0	101.0	1.614	102.2	309.6	179	131	12.0	3665

^aWith low emissivity surface ($\epsilon \sim 0.4$).

to 6.9-MPa (1000-psi) proof and helium leak tests. Only one of these showed a small leak at the point where the electron beam fusing started and stopped. This was corrected by modifying the weld parameters. Thermal cyclic-induced strains are not a concern because these materials have nearly identical expansion coefficients. The predicted failure mode for this joint is thermal diffusion because it will operate at temperatures up to 1093°C (2000°F). Two joints were subjected to a 1177°C (2150°F) vacuum thermal diffusion cycle for 6 h. Posttest evaluation showed no leaks and the ability to withstand the 6.9-MPa (1000-psi) proof-pressure testing. Under normal engine operation the exhaust gas pressure at this joint location is less than 14 kPa (2 psi).

Injector Validation

Two identical injectors, SN 6-1 and 6-2, were fabricated to reproduce the high performance measured for earlier prototype injectors, SN-1 and SN-2. The reproduced designs were identical except for slightly larger orifice diameters in order to increase the thrust from 440 to 490 N (100 to 110 lbf) without an increase in propellant supply pressures. Table 2 shows the test data from 20 tests that verify the reproducibility of the specific impulse performance of the SN 6-1 and 6-2 injectors when hot-fire tested in the 44:1 bolt-together iridium/rhenium (Ir/Re) chamber. All four injectors SN-1, SN-2, SN 6-1, and 6-2 yielded a specific impulse of 309–310 lbf-s/lbm at the nominal design point. The measured specific impulse as a function of mixture ratio and chamber pressure, using two injectors of the same design and orifice dimensions, are shown in Figs. 3 and 4. The ability to produce two identical high-performance injectors in a lot size of two was a critical programmatic issue that was satisfactorily resolved.

Ir/Re Chamber Validation

Four 490-N (110-lbf) Ir/Re chambers have been built in lot sizes of two. The first two units³ employed mechanical joints and accommodated mechanically held nozzle extensions to obtain performance and life data at an expansion ratio of 44:1. The first of the second two units has been assembled metallurgically, including the fuel-cooled stainless steel-to-rhenium joint and the rhenium-to-columbium 286:1 nozzle extension. The hot-fire test history of these units is provided in Table 3.

One of these chambers³ has accumulated nearly 5 h of burn time and 87 thermal cycles in the bolt-together configuration.

Table 3 490-N Ir/Re chamber test history

Chamber	Burn time, s	Thermal cycles
SN-1	3,885	61
SN-2	17,194	87
SN-3	986	20
SN-4	New	—

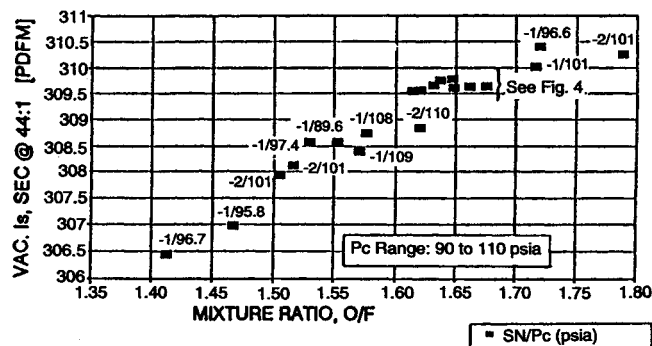


Fig. 3 Vacuum-specific impulse vs mixture ratio for two injectors (S/N 6-1 and S/N 6-2) at area ratio = 44:1.

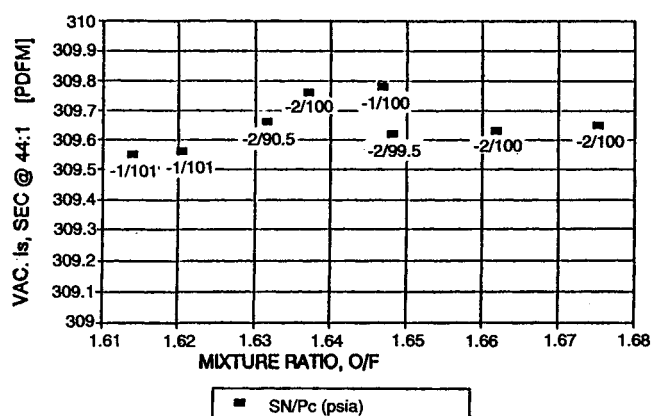


Fig. 4 S/N 6-1 and S/N 6-2 injector vacuum-specific impulse vs mixture ratio at area ratio = 44:1.

Table 4 Test history and performance 490-N Ir-Re thruster-welded area ratio 286:1

Run no.	Firing time, s	Pc, psia	MR, O/F	$^{\circ}\text{F}_{\text{vac}}$, lbf	$I_{\text{sp vac}}$, s	$I_{\text{sp vac}}$ normalized (MR = 1.650), s	Regen. outlet, $^{\circ}\text{F}$	Regen. delta T, $^{\circ}\text{F}$	Regen. heat trans., Btu/s	Chamber temperature, $^{\circ}\text{F}^a$
259	1.0	113.8	1.667	105.6	323.5	—	119	59	—	—
260	5.0	113.6	1.652	109.0	322.0	—	179	120	11.0	—
261	10.0	116.1	1.639	112.4	323.2	323.3	183	124	11.7	2777
262	10.0	127.4	1.592	122.8	320.2	321.0	168	108	11.6	2707
263	10.0	104.7	1.620	100.3	321.2	321.5	200	142	12.3	2934
264	10.0	117.3	1.599	113.0	321.1	321.8	175	117	11.4	3033
265	25.0	116.1	1.647	112.2	322.2	322.3	193	134	12.8	—
266	25.0	126.9	1.636	122.9	321.7	321.9	178	119	12.5	3171
267	23.0	104.8	1.624	100.6	321.3	321.6	210	151	13.1	3381
268	25.0	116.2	1.461	111.0	318.0	322.3	176	118	12.1	3124
269	25.0	115.9	1.789	112.2	321.8	322.0	207	149	13.6	3378
270	5.0	107.8	1.588	102.6	319.3	320.1	178	120	10.8	2626
271	60.0	114.8	1.594	110.7	321.6	322.4	193	133	12.7	3251
272	100.0	113.5	1.581	109.2	320.8	321.8	194	135	12.9	3259
273	120.0	113.7	1.587	109.8	321.8	322.7	195	136	13.0	3263
274	120.0	103.5	1.609	99.5	321.2	321.7	217	157	13.6	3391
275	120.0	116.5	1.514	111.5	318.8	321.4	183	124	12.4	3170
276	120.0	114.8	1.637	110.8	321.5	321.6	200	139	13.2	3288
277	51.7	114.9	1.800	111.2	321.6	322.0	215	153	13.8	3391
278	120.0	127.6	1.672	123.8	321.6	321.4	184	124	12.9	3199

^aWith high emissivity surface ($\epsilon = 1.0$).

Total 985.7 s in 20 firings; average, all tests = 321.8.

Another has accumulated more than 1 h of burn time and 61 thermal cycles, including 17 with a metallurgically joined columbium mini-skirt. A third has been hot-fire tested for 986 s in the full 286:1 engine assembly. None have experienced measurable changes in throat diameter or surface erosion.

Performance Determination

Prediction at Area Ratio of 286:1

Performance measurements made at sea level conditions, area ratios = 1.68:1, and 44:1, were employed to calculate the energy release efficiency. This was determined to be 98.7%. The specific impulse was then computed for the 286:1 area ratio configuration using JANNAF methodology,⁴ with boundary-layer module (BLM) code inputs compatible with Ref. 5. This analysis resulted in a predicted specific impulse of 320.6 lbf-s/lbm.

Performance Test Results at Area Ratio of 286:1

Twenty tests at simulated altitude conditions were conducted in the prototype all-welded configuration. The test results are given in Table 4.

The thrust- and flow-based specific impulse data from the 120-s duration tests are shown in Fig. 5 as a function of mixture ratio and in Fig. 6 as a function of thrust level. These were obtained by varying the propellant tank pressures for each test. The measured specific impulse at the nominal operating mixture ratio of 1.65 is 321.6 lbf-s/lbm (± 0.5 s 1σ). As noted in these figures, there is little sensitivity to propellant supply pressures.

Stability

All of the tested engine assemblies include a critically damped acoustic resonator cavity as part of the injector design. None of the engines tested to date have shown evidence of combustion instability over the wide test range employed.

Thermal Performance

Thermal performance is measured by the maximum temperature of the chamber that is found a short distance upstream of the throat, the temperatures at the bimetallic joints, the fuel temperature leaving the regeneratively cooled chamber forward end, and the postfire heat-soak temperatures.

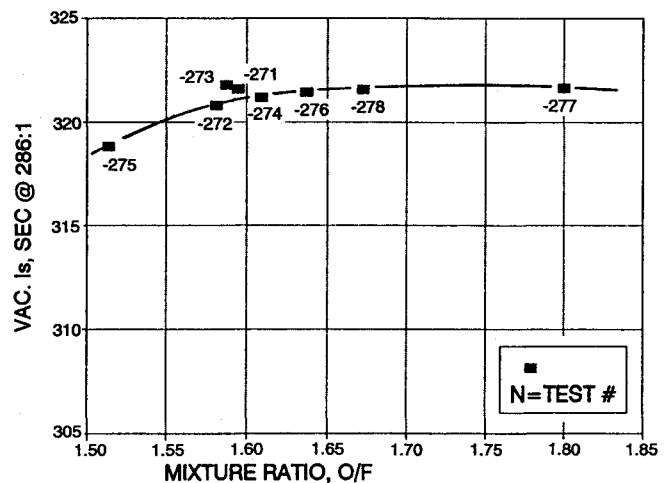


Fig. 5 286:1 vacuum-specific impulse vs mixture ratio.

Figure 7 shows the maximum temperature as a function of engine mixture ratio and chamber pressure. These are less than 1871°C (3400°F), which is 333°C (600°F) below the 2204°C (4000°F) capability of the design and the material.

Figure 8 shows the measured temperature at the upstream and downstream sides of the rhenium-to-columbium joint as a function of time. Steady-state values are noted after 30 s with little sensitivity to operating conditions.

The fuel regenerative coolant discharge temperatures, shown in Fig. 9 as a function of mixture ratio, are well below the boiling point of MMH, 191°C (375°F), at the operating pressure of 1.38 MPa (200 psi) and below the design limit of 204°C (400°F).

Performance Predictions for Other Area Ratios

Table 5 provides the expected performance as a function of overall engine length and area ratio.

Test Facility, Measurements, and Accuracy

The 44:1 and 286:1 area ratio engine configurations were tested in the Aerojet space simulation test facility located in Sacramento, California. Table 6 provides a listing of the crit-

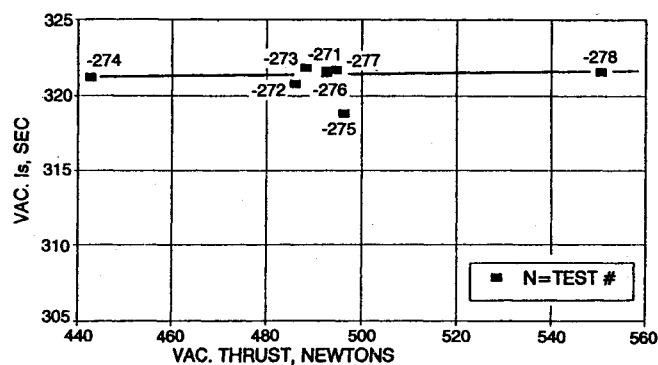


Fig. 6 286:1 vacuum-specific impulse vs engine thrust.

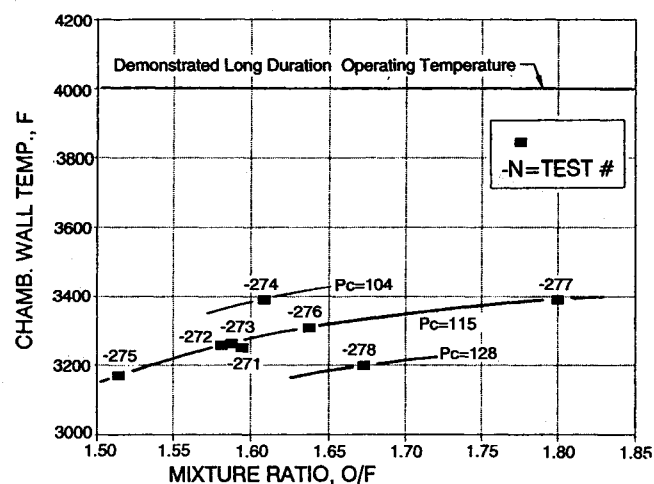


Fig. 7 Maximum chamber temperature vs mixture ratio.

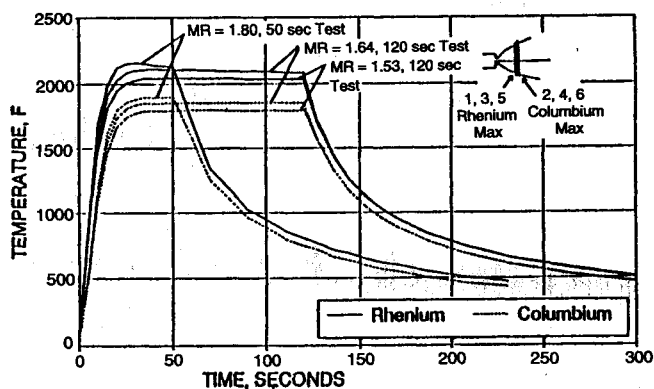


Fig. 8 Rhenium-to-columbian joint temperature.

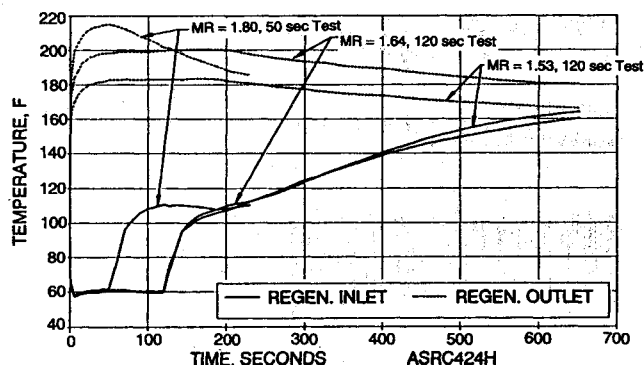


Fig. 9 Welded 286:1 iridium-rhenium engine fuel cooling circuit inlet and outlet temperature vs time.

Table 5 Specific impulse vs engine area ratio and length

Area ratio	Length, cm (in.) including valve	I_{sp} lbf-s, lbfm
44:1	36.8 (14.5)	309.5 ^a
170:1	61.5 (24.2)	319.6 ^b
286:1	69.8 (27.5)	321.6 ^a
400:1	85.0 (33.5)	324 ^b

^aDemonstrated. ^bCalculated.

Table 6 Critical instrumentation

Measurement type	Sensor	Range	Accuracy, 1 σ
Flow	Turbine (flow measurement system model FT-4-8A)	0.08–0.22 lbfm/s	0.14%
Thrust	Strain gauge load cell (Lebow model 3397)	0–200 lbf	0.193%
Cell pressure	Barocell (MKS Baratron model 220BHS-4A1-B-10)	0–10,000 μ m	0.27%

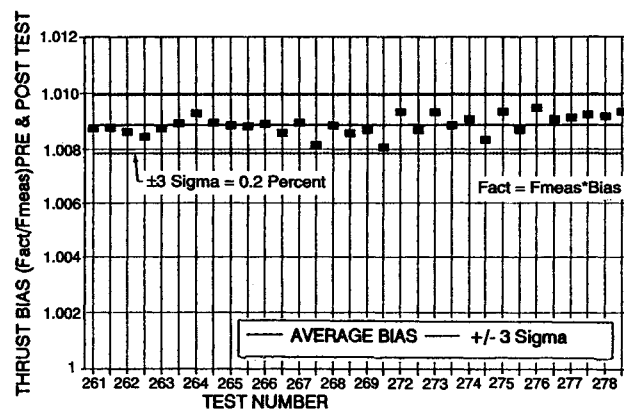


Fig. 10 Thrust stand bias and repeatability measurements.

ical instrumentation and the expected 1σ measurement error. All of the critical performance measurement parameters, i.e., propellant flow rate, thrust, and vacuum cell pressure, are redundant. The turbine-type flow meters are calibrated in place on the test stand, with propellants, using positive displacement flow meters with stroke-position times bore area traced to the National Bureau of Standards (NBS). Similarly, the dual-bridge thrust measurement load cells are dead-weight calibrated. The cell pressure is measured with two Baratron model 220BHS-4A1-B-10, plus two 1-psia strain gauge transducers. On-line pre- and postfire calibrations are conducted in vacuum with the propellant lines pressurized. Multiple force loadings are applied to the engine thrust frame using an automated pneumatic actuation system. This external force along the engine thrust centerline results in the thrust measuring cells and reference standard loaded in series. The difference in force resulting from the attachment of the propellant feed lines and instrumentation is used to define the "system bias." The unique nature of the Aerojet thrust stand design makes this correction a very small and highly repeatable value as demonstrated in Fig. 10.

Temperatures are measured by thermocouples up to 1204°C (2200°F) and two-color optical pyrometers for temperatures greater than 1093°C (2000°F).

Economic Benefits

The economic benefits to be derived from this advanced class of engine are significant. Figure 11 displays the weight

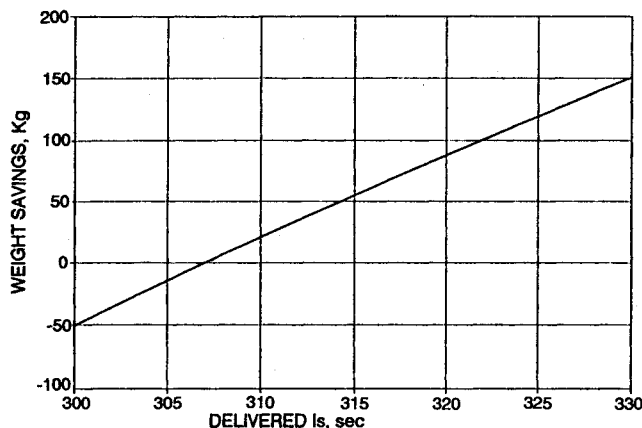


Fig. 11 Higher performance yields significant economic benefits.

savings for a typical INTELSAT 7 class spacecraft. The 185 lb of propellant saved in the high-thrust orbit transfer can extend the useful life of the 12-yr system to 15 yr. Additional savings in weight and/or life extension are achieved when the improved performance of the high-performance lower thrust station-keeping engines are included.^{1,2}

Conclusions

The key to higher performance liquid apogee engines, e.g., $I_{sp}v = 321.6 \pm 0.5 \text{ s } 1\sigma$ [NTO/MMH at $MR = 1.65$, $^\circ F = 490 \text{ N (110 lbf)}$, $P_c = 0.79 \text{ MPa (115 psia)}$, area ratio 286:1] with long life is the unique combination of the Aerojet platelet injector, the elimination of performance loss and exhaust contamination normally associated with fuel film cooling, and the Ir/Re chamber technology.

The technology for the all-welded 490-N liquid apogee engine (LAE) has been demonstrated with a full-scale 286:1 area ratio engine. In addition, key design features of the AJ10-221 have been validated at lower area ratios and in the laboratory with full-scale and subscale specimen, e.g., dissimilar metal joining.

The AJ10-221 is applicable to a wide range of satellite, lunar, and planetary spacecraft propulsion systems and is ready for demonstration/validation, development, and production at this time.

Postscript

Testing of the prototype all-welded engine assembly continued following the original presentation of this work in 1992 at the 28th Joint Propulsion Conference. One engine accumulated 6.3 h of hot-fire time in 93 tests, including one 2-h continuous burn. These results are documented in Ref. 6.

Acknowledgments

The following companies are acknowledged for their contributions: Moog, Inc., valve subcontractor; Ultramet, rhenium chamber subcontractor; Tecomet, columbium skirt subcontractor; NASA Lewis Research Center, project sponsor; and Jet Propulsion Laboratory, Project Support, mission definition.

References

- ¹Rosenberg, S. D., and Schoenman, L., "New Generation of High-Performance Engines for Spacecraft Propulsion," *Journal of Propulsion and Power*, Vol. 10, No. 1, 1994, pp. 40–46.
- ²Lansaw, P. T., and Wooten, J. R., "High Temperature Oxidation Resistant Thruster Research," NASA CR 185233, Feb. 1990.
- ³Schoenman, L., and Franklin, J. E., "Feasibility Demonstration of a High Performance 100-lbf Rocket Engine," Jet Propulsion Lab. Contract 957882, Pasadena, CA, Jan. 1989.
- ⁴JANNAF *Rocket Engine Performance Prediction Manual and Evaluation Manual*, Chemical Propulsion Information Agency Publication 246, Johns Hopkins Applied Physics Lab., Laurel, MD, April 1975.
- ⁵Schoenman, L., and Block, P., "Laminar Boundary-Layer Heat Transfer in Low Thrust Rocket Nozzles," *Journal of Spacecraft and Rockets*, Vol. 5, No. 9, 1968, pp. 1082–1089.
- ⁶Jassowski, D. M., Rosenberg, S. D., and Schoenman, L., "Durability Testing of the AJ10-221 490 N High Performance (321 sec I_{sp}) Engine," AIAA Paper 93-2130, June 1993.